Near Threshold States in Coupled $DD^* - D^*D^*$ Scattering From Lattice QCD

Travis Whyte[1]

[1]Hamilton Mathematics Institute and School of Mathematics, Trinity College Dublin

Based on arxiv:2405.15741 in collaboration with David J. Wilson[2] and Christopher E. Thomas[2]

[2]DAMTP, University of Cambridge

Lattice 2024, University of Liverpool

UNIVERSITY OF CAMBRIDGE

Trinity College Dublin
Coláiste na Tríonóide, Baile Átha Cliath
The University of Dublin

hadspec

LATTICE 2024
LIVERPOOL

The $T_{cc}^{+}(3875)$

- $T_{cc}^{+}(3875)$ was discovered by LHCb in the invariant mass spectrum of $D^0 D^0 \pi^+$
- The mass and width:

$$\delta m = -360 \pm 40^{+4}_{-0}\ keV$$

$$\Gamma = 48 \pm 2^{+0}_{-14}\ keV$$

- Consistent with $J^P = 1^+$, $I = 0$ and quark content $cc\bar{u}\bar{d}$

LHCb 2109.01038, 2109.01056

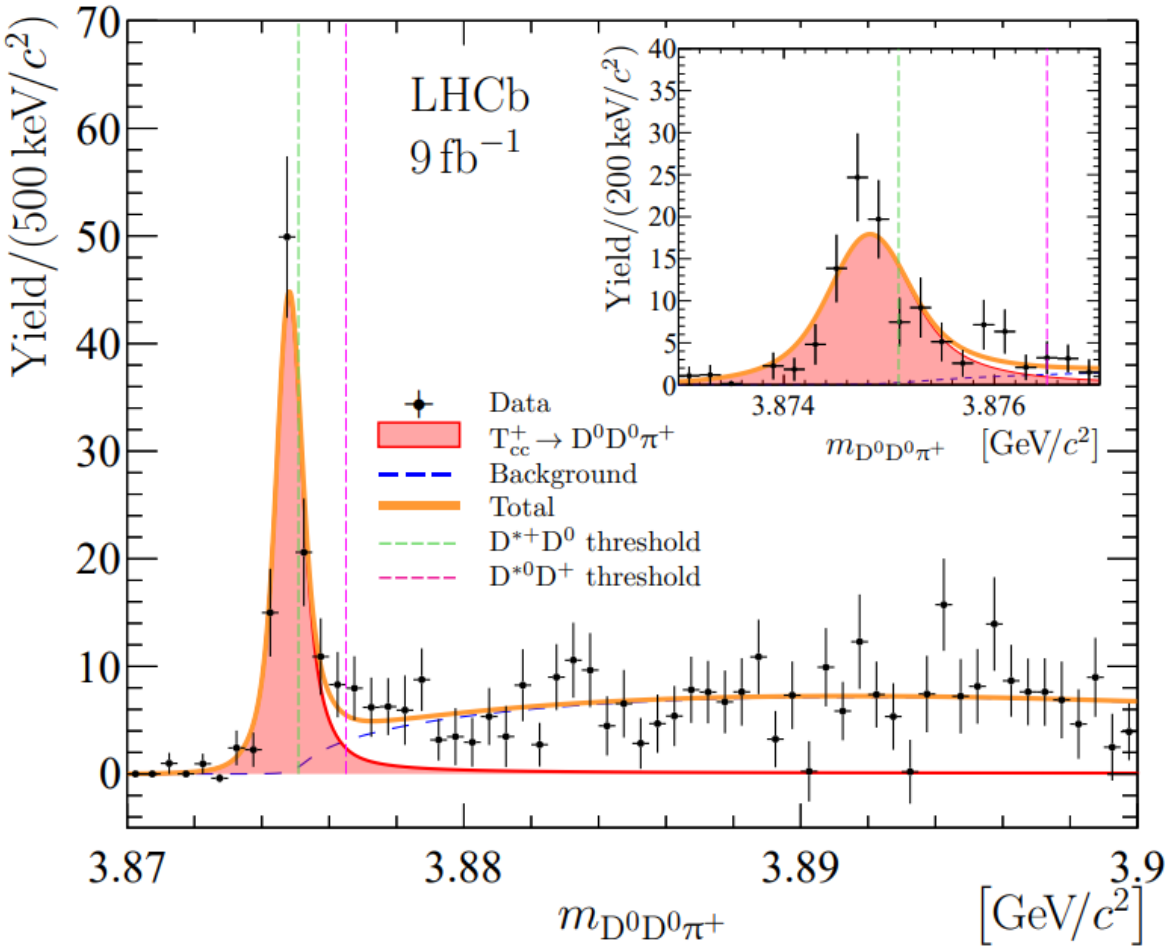

LHCb data ends at 3900 MeV. The $D^{*0} D^{*+}$ channel opens at 4077.11 MeV, which may bring additional features

Previous Work in the DD^* and D^*D^* Channels

- Lattice studies of the T_{cc}
  - Padmanath and Prelovsek 2202.10110
  - Collins et al 2402.14715
  - Lyu et al 2302.04505
  - Ortiz-Pacheco et al 2312.13441
  - Hansen et al 2401.06609
  - Junnarkar et al 1810.12285
  - Chen et al 2206.06185
  - Many others!
- Talks this week on the T_{cc}
  - Parrott Mon 14:15-14:35
  - Basak Mon 14:35-14:55
  - Prelovsek Mon 14:55-15:15
  - Vujmilović Mon 15:15-15:35
  - Dawid Mon 15:35 - 15:55
  - Nagatsuka Thur 9:20-9:40
- Evidence for a state below D^*D^* threshold in $J^P = 1^+$, $I = 0$
  - One gluon exchange Molina et al 1005.0335
  - Hadronic Molecular Models Liu et al 1902.03044
  - Model fits and HQSS M. Albaladejo 2110.02944
  - Chiral EFT Du et al 2110.13765
  - Lattice doubly charmed spectrum Cheung et al 1709.01417
  - Many others!

Details of the Calculation

- Anisotropic "HadSpec" lattices

  Edwards et al 0803.3960, Lin et al 0810.3588

  - $N_f = 2 + 1$ with quenched charm quark
  - Wilson-Clover action
  - $L/a_s = [16, 20, 24]$

- Distillation used for quark field smearing

  Peardon et al 0905.2160

- Meson-meson operators:

  Dudek et al 1212.0830, Dudek et al 1203.6041

$$\mathcal{O}^{\dagger}_{D^{(*)}D^*}(\vec{P}) = \sum_{\vec{p_1},\vec{p_2}} \mathcal{C}(\vec{P};\vec{p_1},\vec{p_2})\Omega^{\dagger}_{D^{(*)}}(\vec{p_1})\Omega^{\dagger}_{D^*}(\vec{p_2})$$

- Calculate spectrum for rest and moving frames
- Connect finite volume energies with Lüscher determinant condition:

  M. Lüscher, Nucl. Phys. B354, Hansen and Sharpe 1204.0826, Briceño and Davoudi 1204.1110 and many others...

- Search the scattering amplitudes for poles

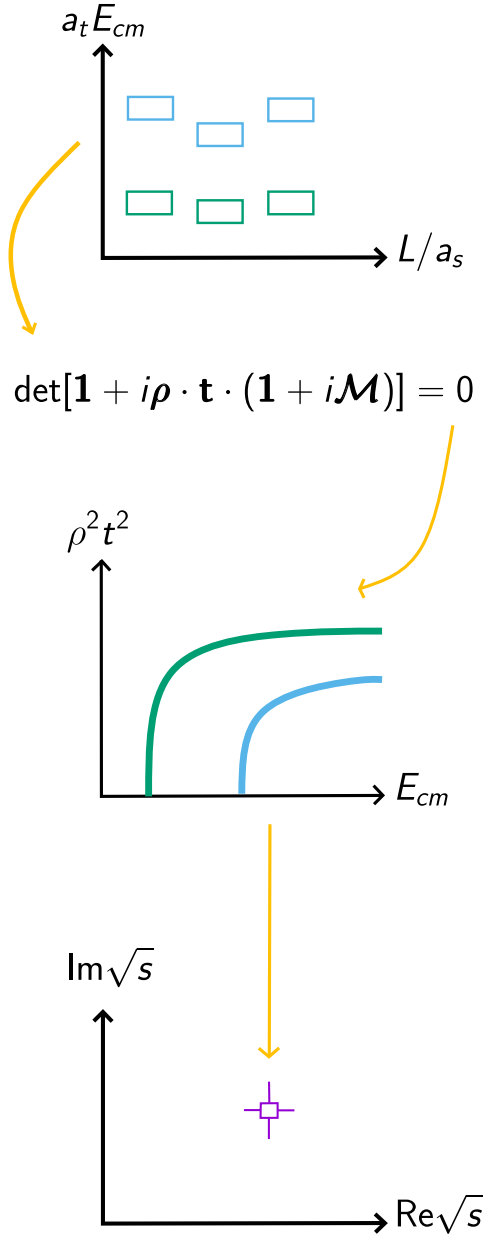

Finite Volume Spectrum $\sim J^P = 1^+$

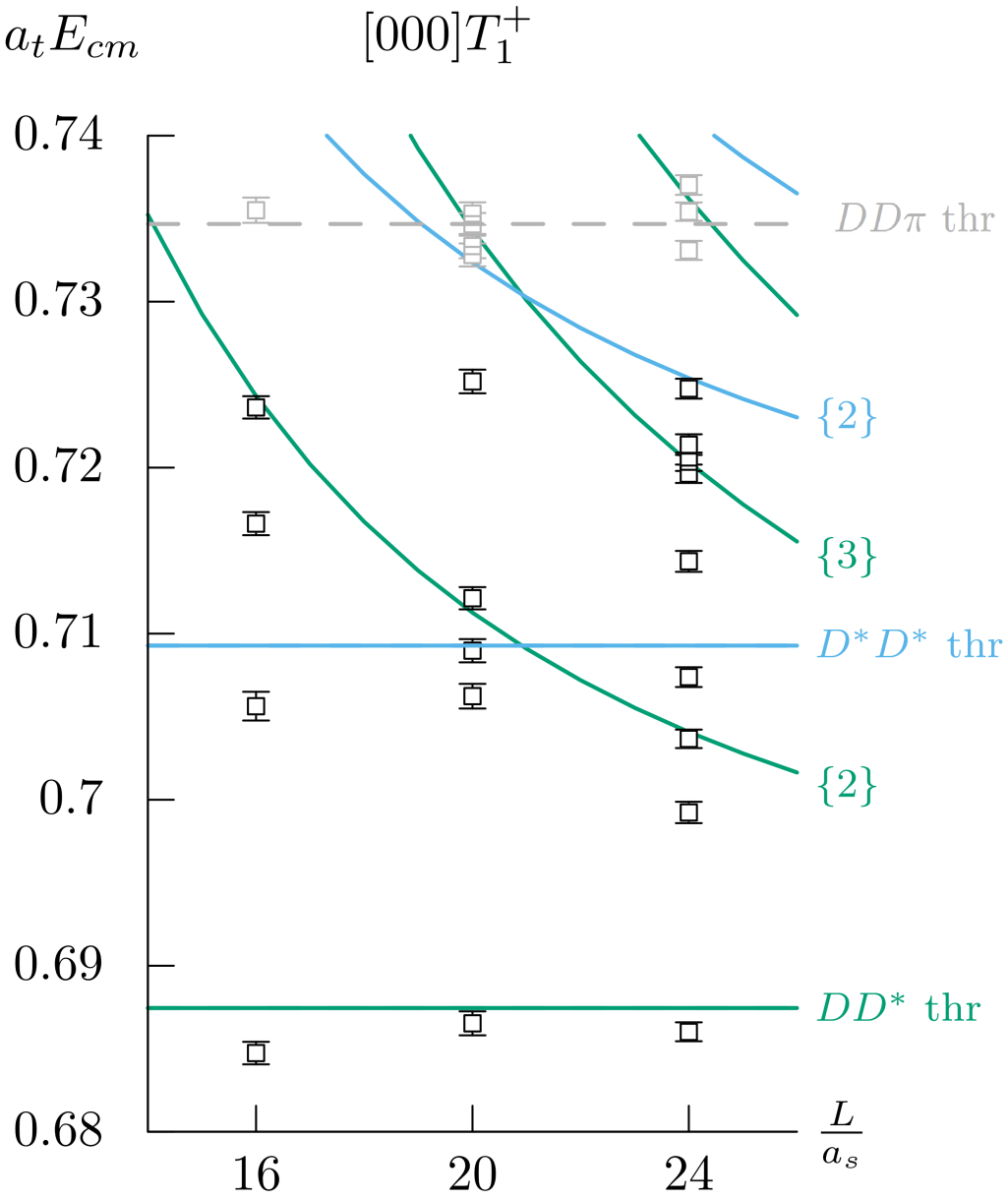

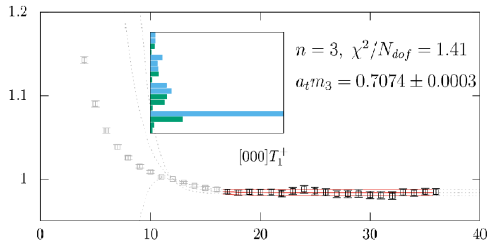

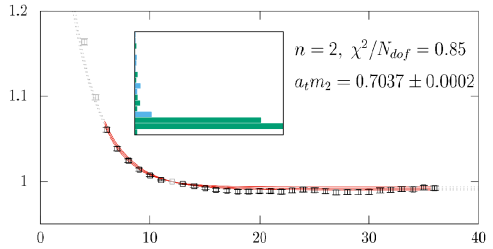

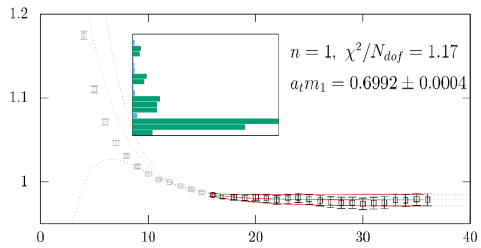

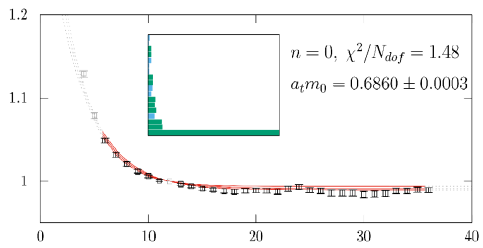

Scattering Below D^*D^* Threshold

$$t^{-1} = K^{-1} + I \qquad \mathrm{Im} I_{ij} = -\rho_i = 2k_i/\sqrt{s}$$

$$K(s)_{\ell SJa,\ell' S' Jb} = \sum_n \gamma^{(n)}_{\ell SJa,\ell' S' Jb} s^n$$

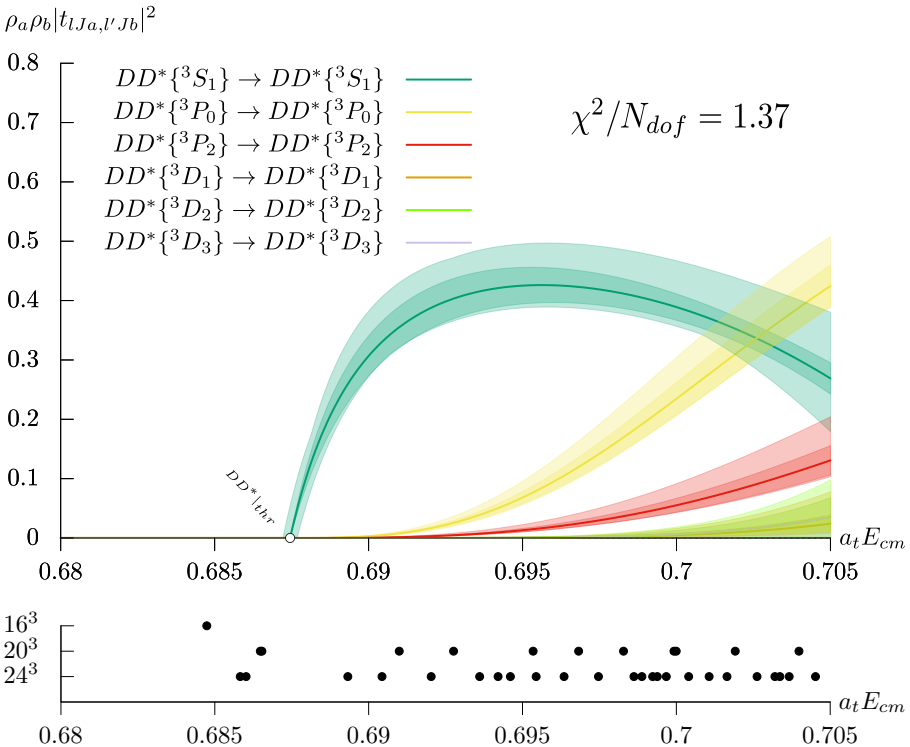

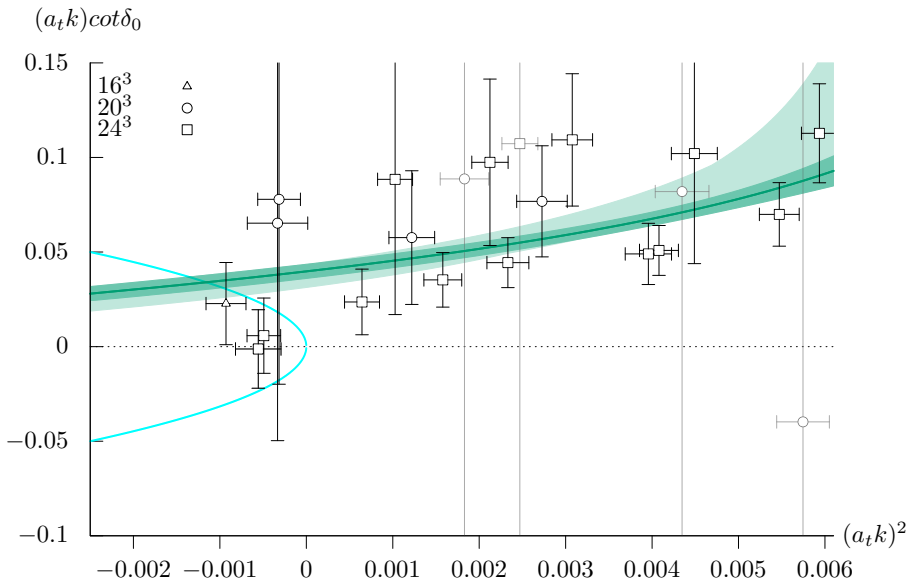

$$t = \frac{E_{cm}}{2} \frac{1}{kcot\delta_0 - ik}$$

Coupled Channel DD^*-D^*D^* Scattering

$$K = \begin{bmatrix} \gamma_{DD^* \to DD^*} & \gamma_{DD^* \to D^*D^*} \\ \gamma_{DD^* \to D^*D^*} & \gamma_{D^*D^* \to D^*D^*} \end{bmatrix} + \begin{bmatrix} \gamma_{DD^* \to DD^*} & 0 \\ 0 & \gamma_{D^*D^* \to D^*D^*} \end{bmatrix} s$$

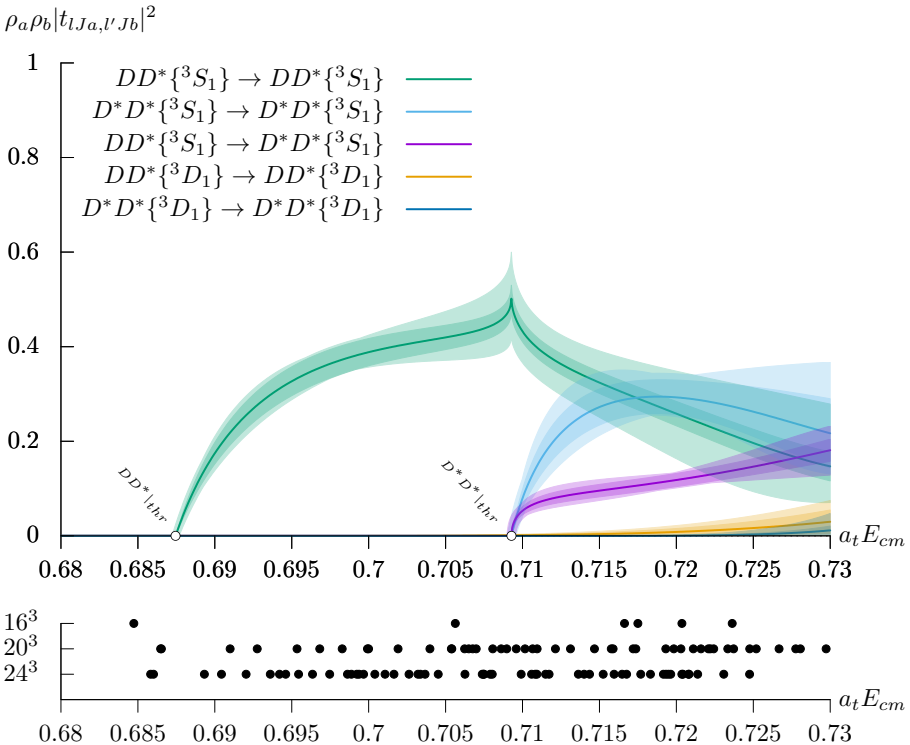

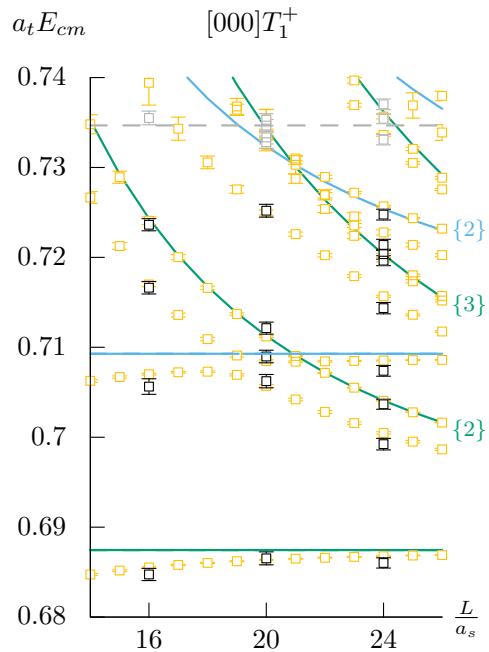

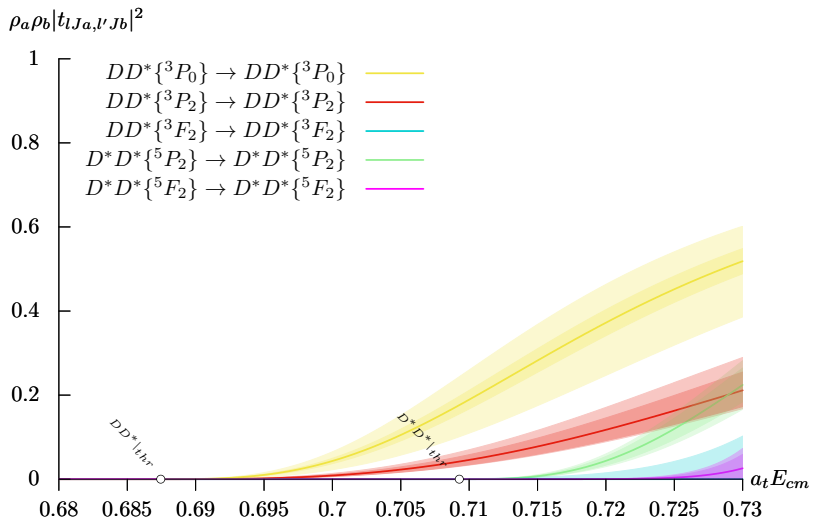

$$\chi^2/N_{dof} = 1.28$$

$$\gamma_{DD^* \to D^*D^*} = 4.11 \pm 0.51 \pm 0.94$$

Coupled Channel DD^*-D^*D^* Scattering

- Additional parameterizations performed to reduce bias

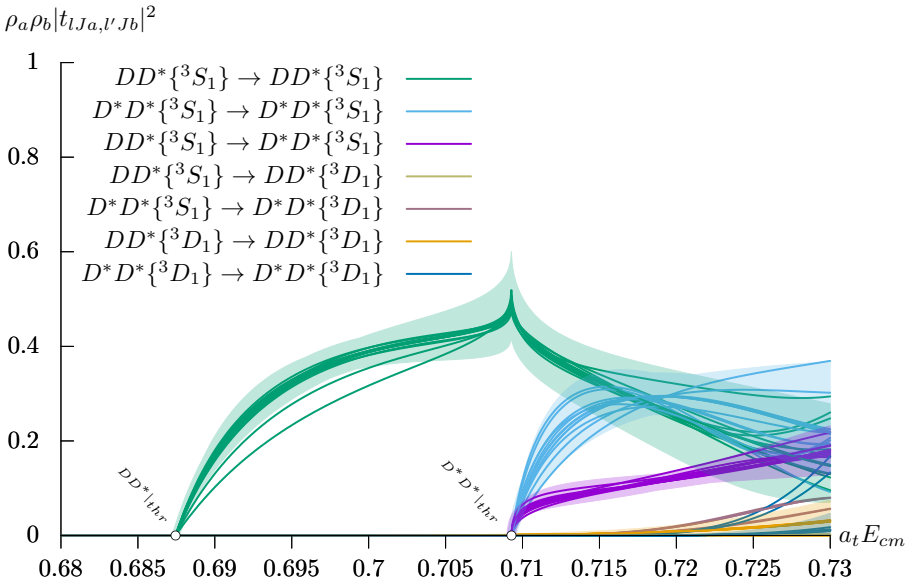

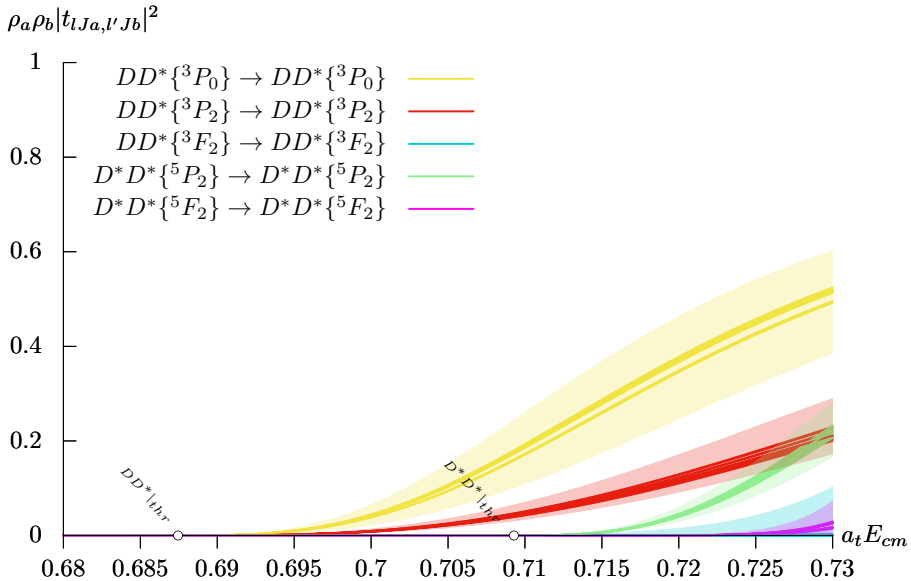

- All successful parameterizations feature a cusp in DD^* S-wave amplitude and non zero coupling in S-wave
- S-wave and D-wave mixing negligible

Poles in the $J^P = 1^+$ Scattering Amplitudes

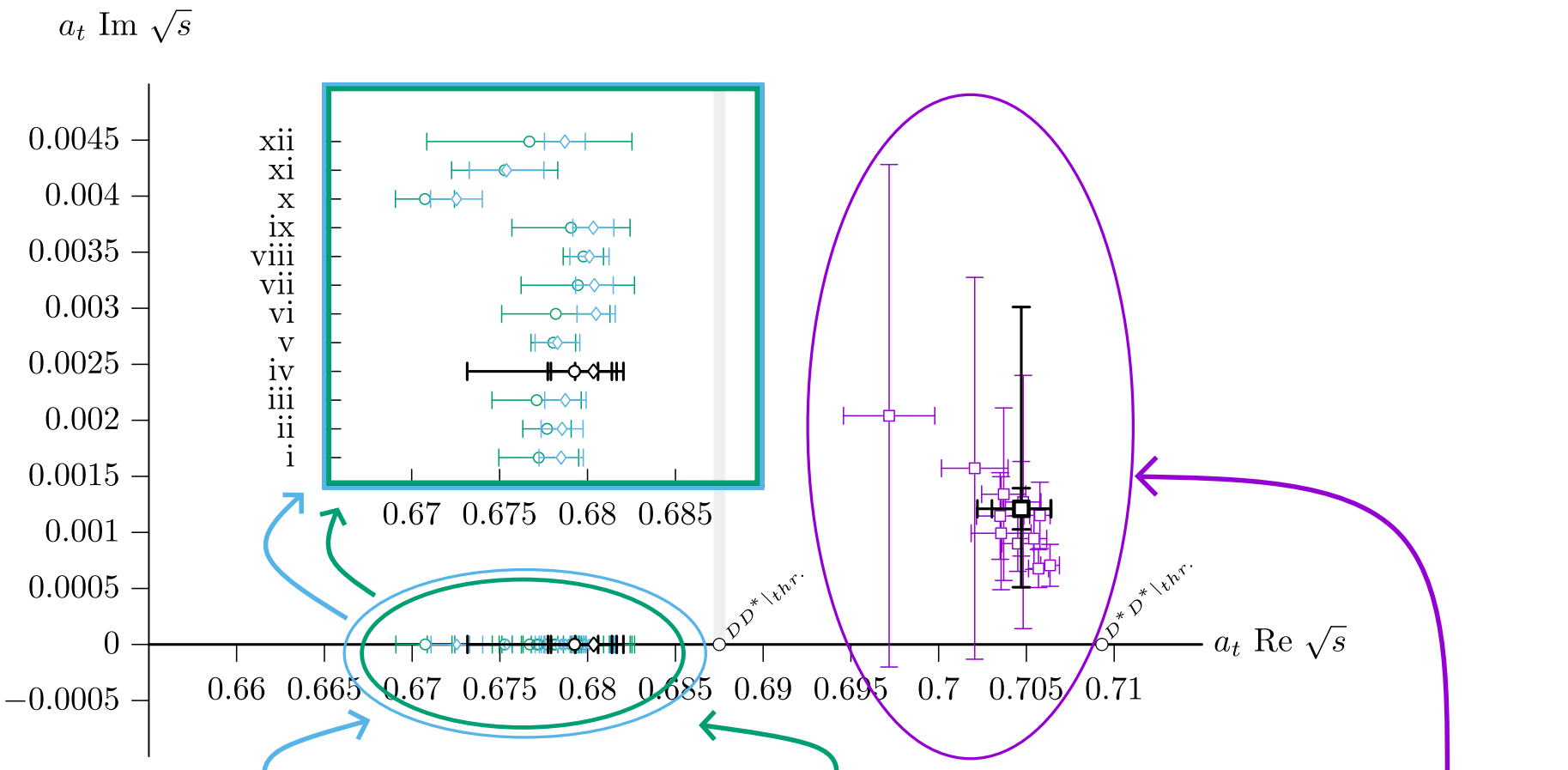

$$a_t\sqrt{s_{\mathrm{II}}} = 0.6765(55) = 3834(31)\ \mathrm{MeV}$$

$$a_t\sqrt{s_{\mathrm{III}}} = 0.6759(68) = 3830(40)\ \mathrm{MeV}$$

$$a_t\sqrt{s_{\mathrm{IV}}} = 0.7007(62) + \frac{i}{2}(0.0020(22)) = 3971(35) + \frac{i}{2}11(13)\ \mathrm{MeV}$$

Poles in the $J^P = 1^+$ Scattering Amplitudes

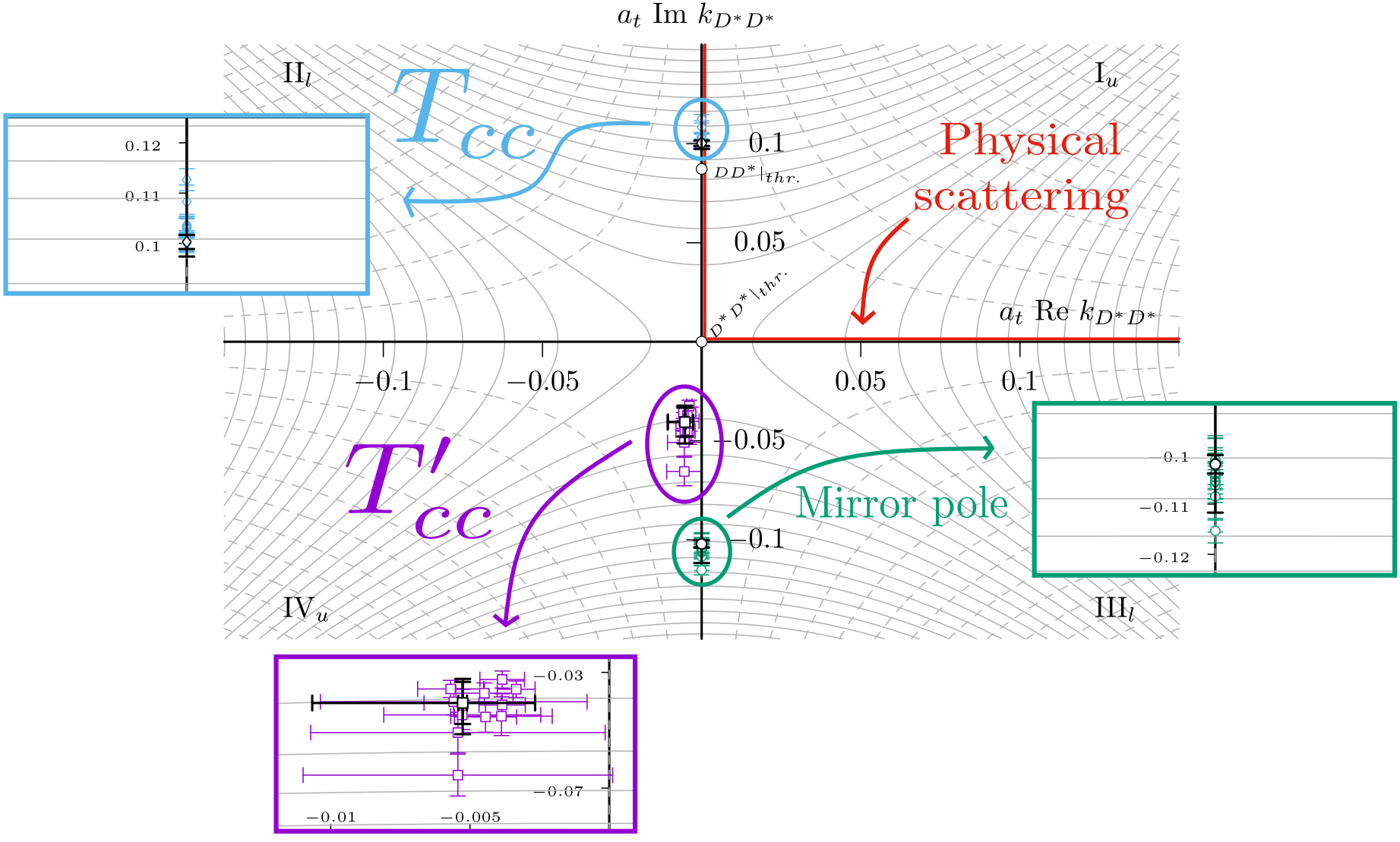

Poles in the $J^P = 1^+$ Scattering Amplitudes - Couplings

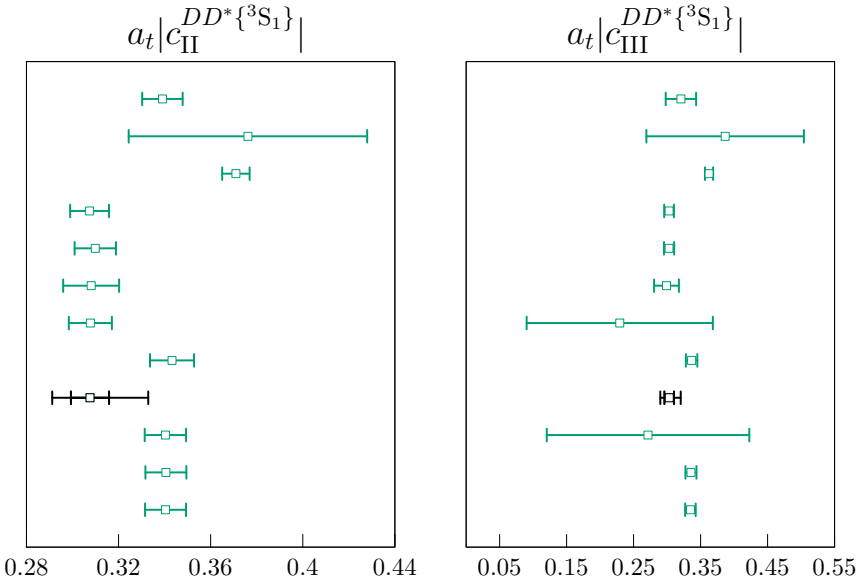

$$a_t c_{\mathrm{IV}}^{DD^*\{^3S_1\}} = -0.07(4) + i(0.10(7))$$
$$|c_{\mathrm{IV}}^{DD^*\{^3S_1\}}| = 692(195)\,\mathrm{MeV}$$
$$a_t c_{\mathrm{IV}}^{D^*D^*\{^3S_1\}} = 0.00(4) + i(0.33(8))$$
$$|c_{\mathrm{IV}}^{D^*D^*\{^3S_1\}}| = 1870(450)\,\mathrm{MeV}$$

$$a_t c_{\mathrm{II}}^{DD^*\{^3S_1\}} = i(0.36(7))$$
$$|c_{\mathrm{II}}^{DD^*\{^3S_1\}}| = 2040(400)\,\mathrm{MeV}$$
$$a_t c_{\mathrm{III}}^{DD^*\{^3S_1\}} = i(0.30(21))$$
$$|c_{\mathrm{III}}^{DD^*\{^3S_1\}}| = 1700(1200)\,\mathrm{MeV}$$

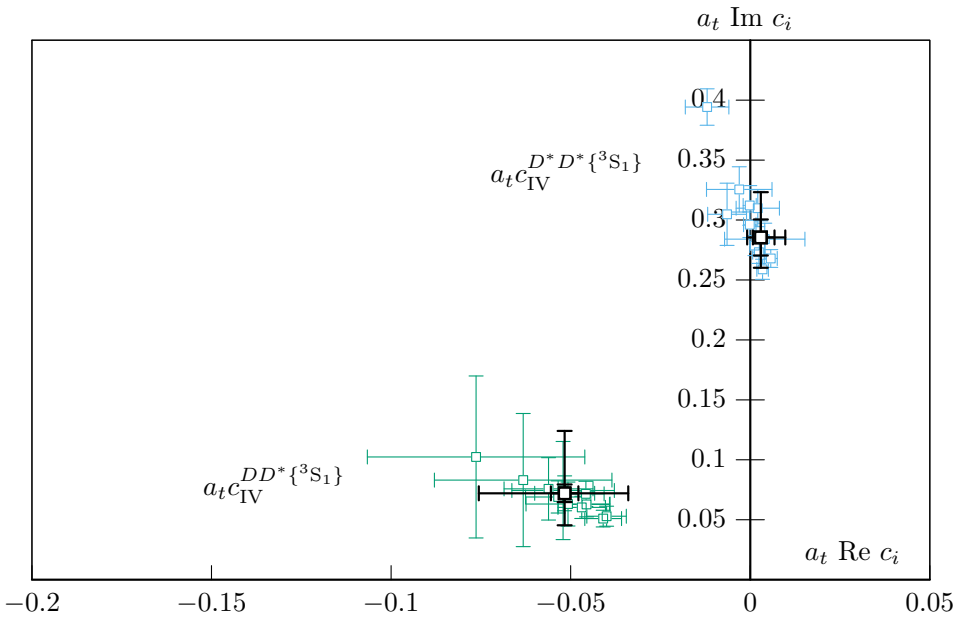

Exploring the $DD^* \to D^*D^*$ Coupling

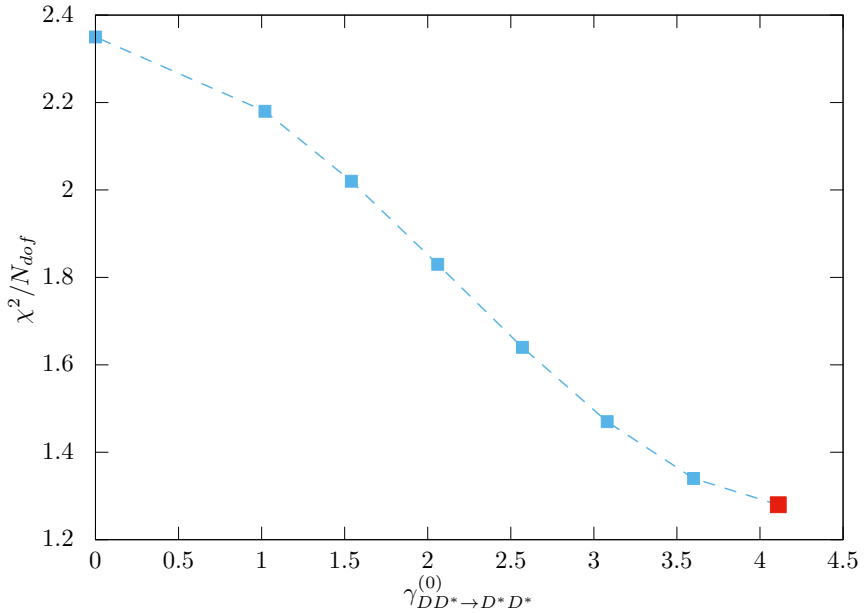

- As coupling is decreased, cusp at D^*D^* threshold disappears
- D^*D^* S-wave amplitude is correspondingly enhanced

- As the matrix element coupling the two channels in S-wave decreases, the χ^2 increases
- Suggests an incompatibility of the spectrum with zero coupling

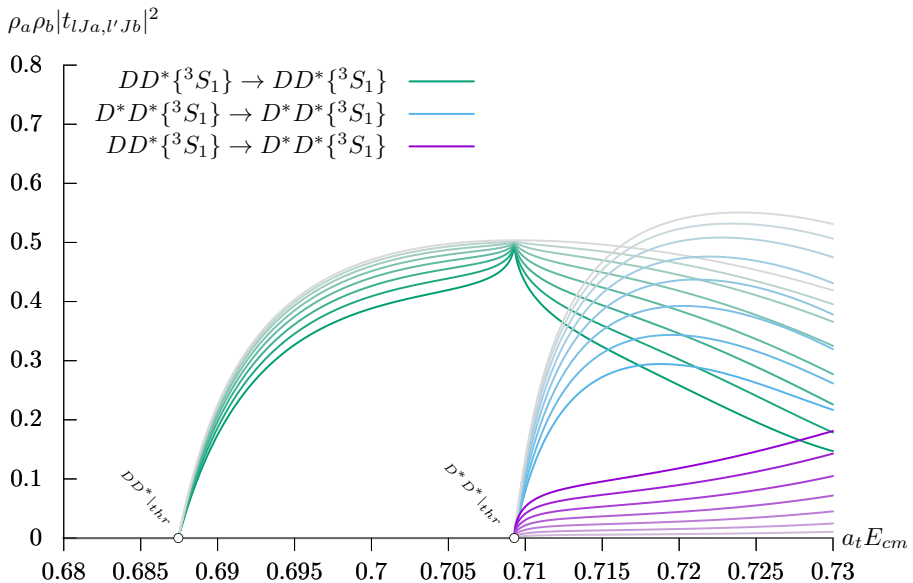

Exploring the $DD^* \to D^*D^*$ Coupling

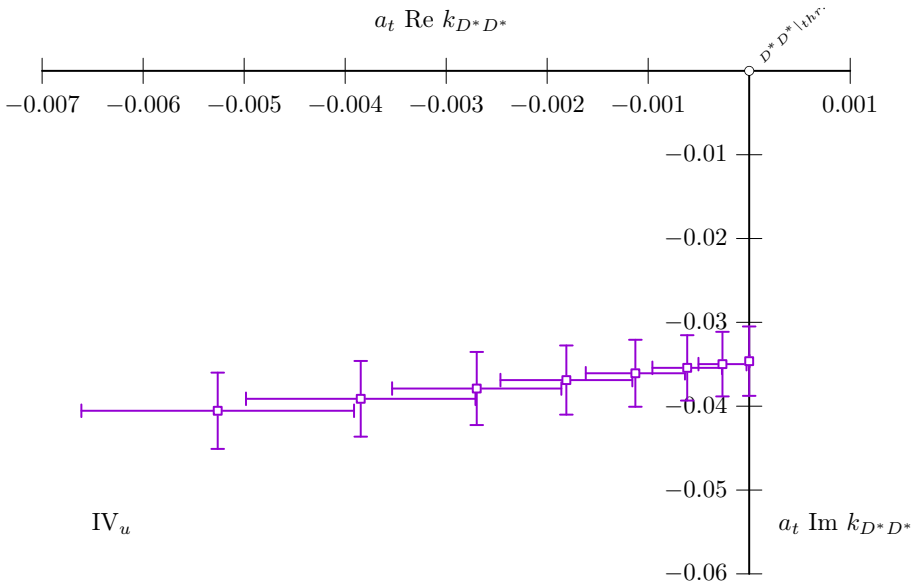

- Resonance becomes a virtual bound state in the limit that the channels are decoupled

- As the coupling is decreased, the pole position moves on axis in the momentum and energy planes

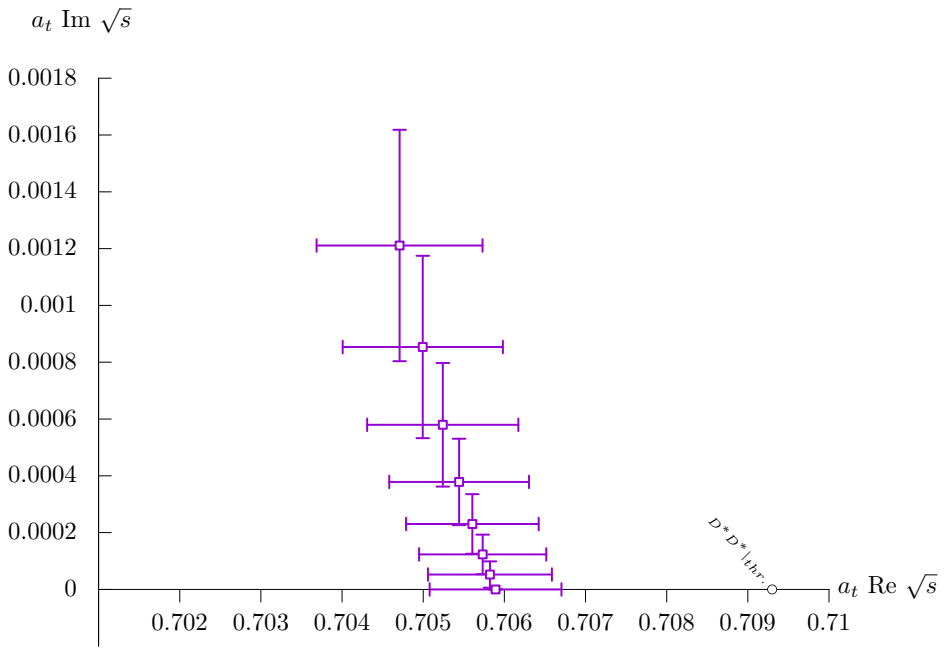

Summary and Outlook

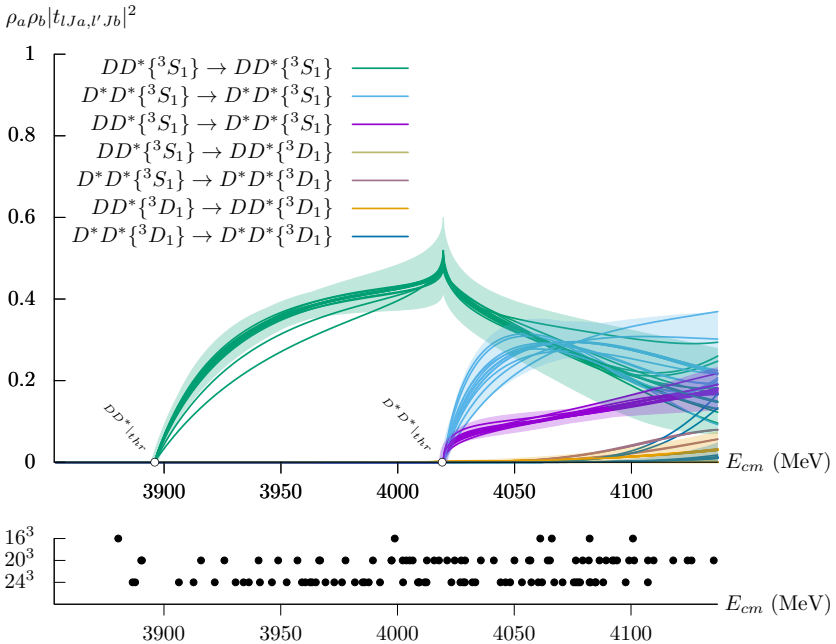

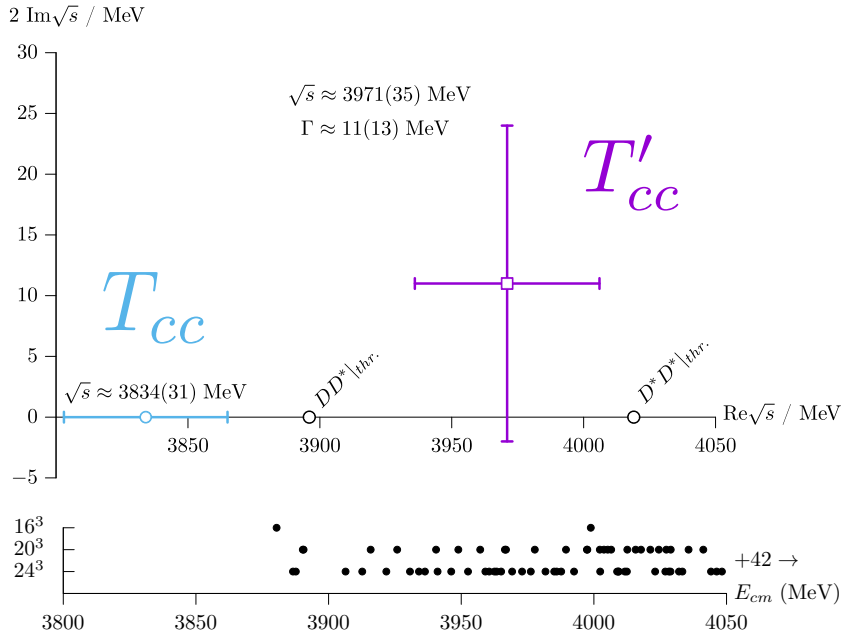

- Two states are observed in the DD^* and D^*D^* S-wave amplitudes
  - The virtual bound state $T_{cc} \sim 62$ MeV below DD^* threshold
  - The as yet unobserved resonance $T'_{cc} \sim 49$ MeV below the D^*D^* threshold
- The T'_{cc} should be observable in the DD^* and D^*D^* final states of ongoing experiments investigating the $I = 0$, $J^P = 1^+$ doubly charmed sector

Acknowledgments

- Thank you to my collaborators for all of their help and guidance in this project
- This work funded through the Royal Society, UKRI STFC and Science Foundation Ireland
- Calculations performed on DiRAC and Jefferson Lab compute facilities
- Thank you for your attention!

THE ROYAL SOCIETY

Jefferson Lab

Science and Technology Facilities Council

had spec

DiRAC
High Performance Computing Facility

LATTICE 2024
LIVERPOOL

Details of the Calculation

$(L/a_s)^3 \times (T/a_t)$	N_{cfgs}	N_{tsrcs}	N_{vecs}
$16^3 \times 128$	478	8	64
$20^3 \times 256$	288	3-4	128
$24^3 \times 128$	553	3-4	160

	$a_t m$	m (MeV)
π	0.06906(13)	391(1)
DD	0.33281(9)	1886(1)
DD*	0.35464(14)	2010(1)

	$a_t m$	m (Mev)
DD^*	0.68745(17)	3896(1)
D^*D^*	0.70928(20)	4020(1)
$DD\pi$	0.73468(18)	4163(1)

- Calculations performed on three anisotropic lattices of spatial extent $a_s \approx 0.12$ fm with $\xi = a_s/a_t \approx 3.444(50)$ Edwards et al 0803.3960, Lin et al 0810.3588
- Distillation used to smear the quark fields and efficiently calculate all necessary Wick contractions Peardon et al 0905.2160
- Ω baryon used to set the scale with $m^{\Omega}_{phys}/a_t m_{\Omega} = 5667$ MeV Edwards et al 1212.5236

Details of the Calculation

- Finite volume energy levels are extracted by solving the GEVP Dudek et al 1004.4930

$$C_{ij}(t)v_j^{\mathfrak{n}}(t) = \lambda_{\mathfrak{n}}(t,t_0)C_{ij}(t_0)v_j^{\mathfrak{n}}(t) \tag{1}$$

where C is the matrix of correlation functions

$$C_{ij}(t) = \langle 0|\mathcal{O}_i(t)\mathcal{O}_j^{\dagger}(0)|0\rangle. \tag{2}$$

- The principal correlator, $\lambda_{\mathfrak{n}}(t,t_0)$, is used to obtain the energy $E_{\mathfrak{n}}$ of the $\mathfrak{n}^{th}$ eigenstate $|\mathfrak{n}\rangle$

$$\lambda_{\mathfrak{n}}(t,t_0) = (1-A_{\mathfrak{n}})e^{-E_{\mathfrak{n}}(t-t_0)} + A_{\mathfrak{n}}e^{-E_{\mathfrak{n}}^{'}(t-t_0)} \tag{3}$$

and the eigenvectors of the GEVP are used to construct variationally optimized operators $\Omega_{\mathfrak{n}}^{\dagger} = \sum_i v_i^{\mathfrak{n}}\mathcal{O}_i^{\dagger}$ and define the operator overlaps

$$Z_i^{\mathfrak{n}} = \langle \mathfrak{n}|\mathcal{O}_i(0)|0\rangle \tag{4}$$

$$= \sqrt{2E_{\mathfrak{n}}}e^{(E_{\mathfrak{n}}t_0)/2}(v_j^{\mathfrak{n}})^* C_{ji}(t_0). \tag{5}$$

Interpolating Operators

- The finite volume of the lattice breaks the rotational symmetry of the infinite volume continuum
- Hadrons at rest with definite continuum momentum J are projected to the finite cubic irreducible representation (irrep), Λ, which is called *subduction* Dudek et al 1004.4930
- Utilize only meson-meson operators of the form Dudek et al 1212.0830, Dudek et al 1203.6041

$$\mathcal{O}^{\Lambda\,\dagger}_{D^{(*)}D^*}(\vec{P}) = \sum_{\vec{p_1},\vec{p_2}} \mathcal{C}(\vec{P}\Lambda;\vec{p_1}\Lambda_1;\vec{p_2}\Lambda_2) \times \Omega^{\Lambda_1\,\dagger}_{D^{(*)}}(\vec{p_1})\Omega^{\Lambda_2\,\dagger}_{D^*}(\vec{p_2}) \tag{6}$$

where the operators $\Omega_{D^{(*)}}$ are variationally optimized single $D^{(*)}$ meson operators subduced to Λ_1 and Λ_2

$$\Omega \sim \bar{\psi}\Gamma\overleftrightarrow{D}\ldots\overleftrightarrow{D}\Gamma\psi \tag{7}$$

D^*D^* Symmetry Considerations

- Bose symmetry dictates that the overall wavefunction of D^*D^* be symmetric

		D^*D^*				
ℓ	$^{2S+1}\ell_J$	J^P	Spin	Space	Flavor	Total
0	$^3S_1$	1^+	A	S	A	S
1	$^1P_1$ $^5P_{1,2,3}$	1^- $\{1,2,3\}^-$	S	A	A	S
2	$^3D_{1,2,3}$	$\{1,2,3\}^+$	A	S	A	S
3	$^1F_3$ $^5F_{1,\ldots,5}$	3^- $\{1,2,3,4,5\}^-$	S	A	A	S

- No such symmetry requirements for DD^*

	DD^*	
ℓ	$^{2S+1}\ell_J$	J^P
0	$^3S_1$	1^+
1	$^3P_{0,1,2}$	$\{0,1,2\}^-$
2	$^3D_{1,2,3}$	$\{1,2,3\}^+$
3	$^3F_{2,3,4}$	$\{2,3,4\}^-$

Subduction Tables for Mesons at Rest

Pseudoscalar-Vector Scattering for Mesons at Rest Woss et al 1802.05580

Λ^P	T_1^+	A_1^-	E^-	E^+	A_2^+
$J^P(^{2S+1}\ell_J)$	$1^+ \begin{pmatrix} ^3S_1 \\ ^3D_1 \end{pmatrix}$	$0^- \left(^3P_0\right)$			
			$2^- \begin{pmatrix} ^3P_2 \\ ^3F_2 \end{pmatrix}$	$2^+ \left(^3D_2\right)$	
	$3^+ \begin{pmatrix} ^3D_3 \\ ^3G_3 \end{pmatrix}$				$3^+ \begin{pmatrix} ^3D_3 \\ ^3G_3 \end{pmatrix}$
	$4^+ \left(^3G_4\right)$	$4^- \begin{pmatrix} ^3F_4 \\ ^3H_4 \end{pmatrix}$	$4^- \begin{pmatrix} ^3F_4 \\ ^3H_4 \end{pmatrix}$	$4^+ \left(^3G_4\right)$	

Identical Vector-Vector Scattering for Mesons at Rest

Λ^P	T_1^+	A_1^-	E^-	E^+	A_2^+
$J^P(^{2S+1}\ell_J)$	$1^+ \begin{pmatrix} ^3S_1 \\ ^3D_1 \end{pmatrix}$				
			$2^- \begin{pmatrix} ^5P_2 \\ ^5F_2 \end{pmatrix}$	$2^+ \left(^3D_2\right)$	
	$3^+ \begin{pmatrix} ^3D_3 \\ ^3G_3 \end{pmatrix}$				$3^+ \begin{pmatrix} ^3D_3 \\ ^3G_3 \end{pmatrix}$
	$4^+ \left(^3G_4\right)$	$4^- \begin{pmatrix} ^5F_4 \\ ^5H_4 \end{pmatrix}$	$4^- \begin{pmatrix} ^5F_4 \\ ^5H_4 \end{pmatrix}$	$4^+ \left(^3G_4\right)$	

Subduction Tables for Mesons Inflight

Pseudoscalar-Vector Scattering for Mesons at Overall Nonzero Momentum

Woss et al 1802.05580

Λ^P	$[00n]A_2$	$[0nn]A_2$	$[nnn]A_2$
$J^P(^{2S+1}\ell_J)$	$0^-\ (^3P_0)$	$0^-\ (^3P_0)$	$0^-\ (^3P_0)$
	$1^+ \begin{pmatrix} ^3S_1 \\ ^3D_1 \end{pmatrix}$	$1^+ \begin{pmatrix} ^3S_1 \\ ^3D_1 \end{pmatrix}$	$1^+ \begin{pmatrix} ^3S_1 \\ ^3D_1 \end{pmatrix}$
		$2^+\ (^3D_2)$	
	$2^- \begin{pmatrix} ^3P_2 \\ ^3F_2 \end{pmatrix}$	$2^- \begin{pmatrix} ^3P_2 \\ ^3F_2 \end{pmatrix}_{[2]}$	$2^- \begin{pmatrix} ^3P_2 \\ ^3F_2 \end{pmatrix}$
	$3^+ \begin{pmatrix} ^3D_3 \\ ^3G_3 \end{pmatrix}$	$3^+ \begin{pmatrix} ^3D_3 \\ ^3G_3 \end{pmatrix}_{[2]}$	$3^+ \begin{pmatrix} ^3D_3 \\ ^3G_3 \end{pmatrix}_{[2]}$
		$3^-\ (^3F_3)$	$3^-\ (^3F_3)$
	$4^- \begin{pmatrix} ^3F_4 \\ ^3H_4 \end{pmatrix}_{[2]}$	$4^- \begin{pmatrix} ^3F_4 \\ ^3H_4 \end{pmatrix}_{[3]}$	$4^- \begin{pmatrix} ^3F_4 \\ ^3H_4 \end{pmatrix}_{[2]}$

Subduction Tables for Mesons Inflight

Identical Vector-Vector Scattering for Mesons at Overall Nonzero Momentum

Λ^P	$[00n]A_2$	$[0nn]A_2$	$[nnn]A_2$
$J^P(^{2S+1}\ell_J)$	$1^+ \begin{pmatrix} {}^3S_1 \\ {}^3D_1 \end{pmatrix}$	$1^+ \begin{pmatrix} {}^3S_1 \\ {}^3D_1 \end{pmatrix}$	$1^+ \begin{pmatrix} {}^3S_1 \\ {}^3D_1 \end{pmatrix}$
		$2^+ ({}^3D_2)$	
	$2^- \begin{pmatrix} {}^5P_2 \\ {}^5F_2 \end{pmatrix}$	$2^- \begin{pmatrix} {}^5P_2 \\ {}^5F_2 \end{pmatrix}_{[2]}$	$2^- \begin{pmatrix} {}^5P_2 \\ {}^5F_2 \end{pmatrix}$
	$3^+ \begin{pmatrix} {}^3D_3 \\ {}^3G_3 \end{pmatrix}$	$3^+ \begin{pmatrix} {}^3D_3 \\ {}^3G_3 \end{pmatrix}_{[2]}$	$3^+ \begin{pmatrix} {}^3D_3 \\ {}^3G_3 \end{pmatrix}_{[2]}$
		$3^- \begin{pmatrix} {}^5P_3 \\ {}^5F_3 \end{pmatrix}$	$3^- \begin{pmatrix} {}^5P_3 \\ {}^5F_3 \end{pmatrix}$
	$4^- \begin{pmatrix} {}^5F_4 \\ {}^5H_4 \end{pmatrix}_{[2]}$	$4^- \begin{pmatrix} {}^5F_4 \\ {}^5H_4 \end{pmatrix}_{[3]}$	$4^- \begin{pmatrix} {}^5F_4 \\ {}^5H_4 \end{pmatrix}_{[2]}$

Finite Volume Energies

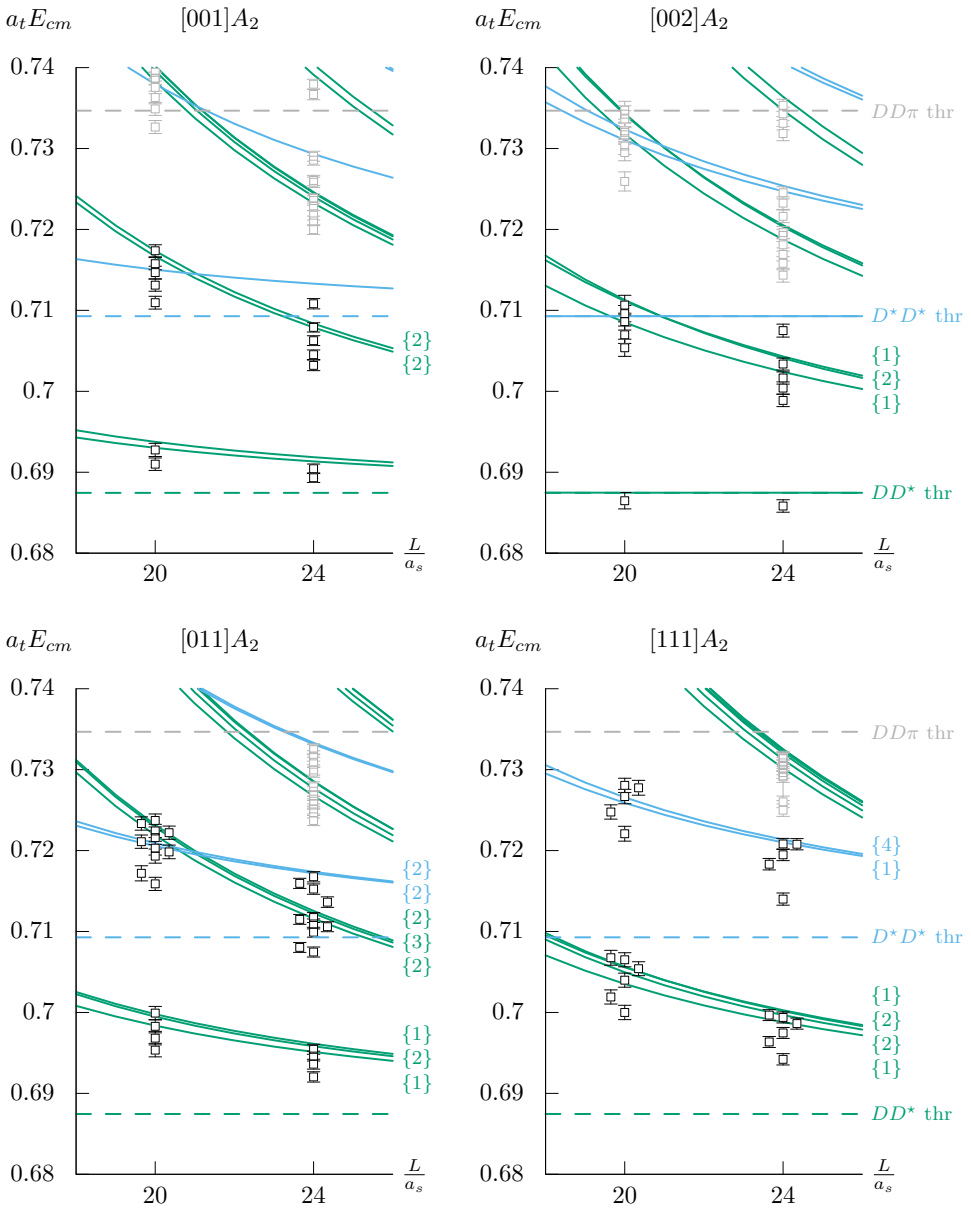

Finite Volume Energies

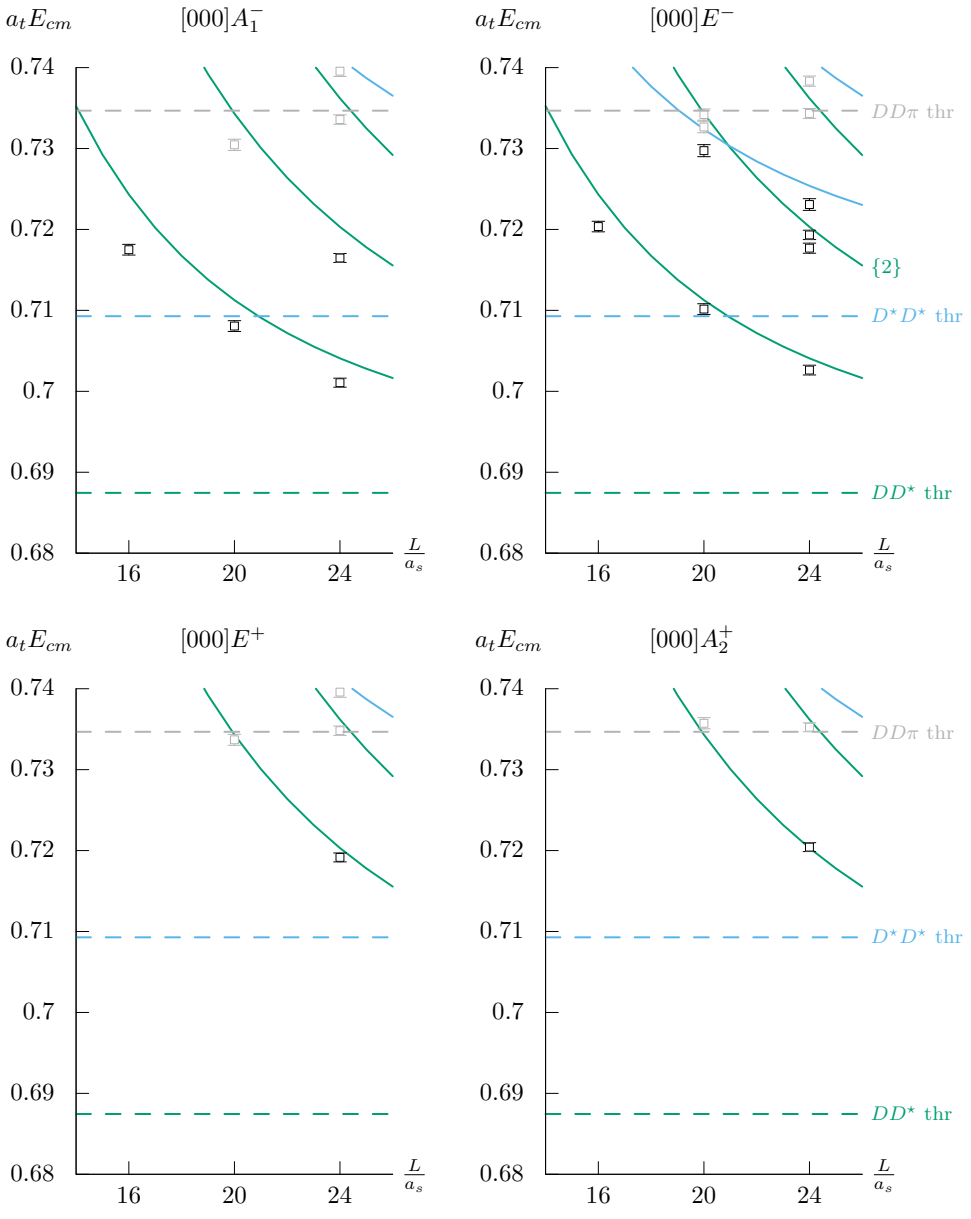

Scattering Analysis

- The Lüscher determinant equation for particles of arbitrary mass and spin M. Lüscher, Nucl. Phys. B354, Hansen and Sharpe 1204.0826, Briceño and Davoudi 1204.1110, Guo et al 1211.0929, and many others...

$$\det[\mathbf{1} + i\boldsymbol{\rho} \cdot \mathbf{t} \cdot (\mathbf{1} + i\boldsymbol{\mathcal{M}})] = 0 \tag{8}$$

  where $\boldsymbol{t}(E_{cm})$ is the infinite volume scattering t-matrix.
- One choice to parameterize $\boldsymbol{t}$ is with a K-matrix parameterization

$$\boldsymbol{t}^{-1} = \boldsymbol{K}^{-1} + \boldsymbol{I} \tag{9}$$

  with matrix elements

$$K(s)_{\ell SJa,\ell' S' Jb} = \sum_n \gamma^{(n)}_{\ell SJa,\ell' S' Jb} s^n \tag{10}$$

Coupled Channel DD^*-D^*D^* Scattering

			D^*D^*			
ℓ	$^{2S+1}\ell_J$	J^P	Spin	Space	Flavor	Total
0	$^3S_1$	1^+	A	S	A	S
1	$^1P_1$ $^5P_{1,2,3}$	1^- $\{1,2,3\}^-$	S	A	A	S
2	$^3D_{1,2,3}$	$\{1,2,3\}^+$	A	S	A	S
3	$^1F_3$ $^5F_{1,\ldots,5}$	3^- $\{1,2,3,4,5\}^-$	S	A	A	S

- Utilizes 109 energy levels up to $a_t E_{cm} = 0.73$
- Starting from elastic DD^* analysis, we make use of all partial waves included there and assume $^3F_2$ is no longer zero
- Explicitly parameterize for D^*D^* $^3S_1$, $^3D_1$, $^5P_2$ and $^5F_2$

Coupled Channel DD^*-D^*D^* Scattering

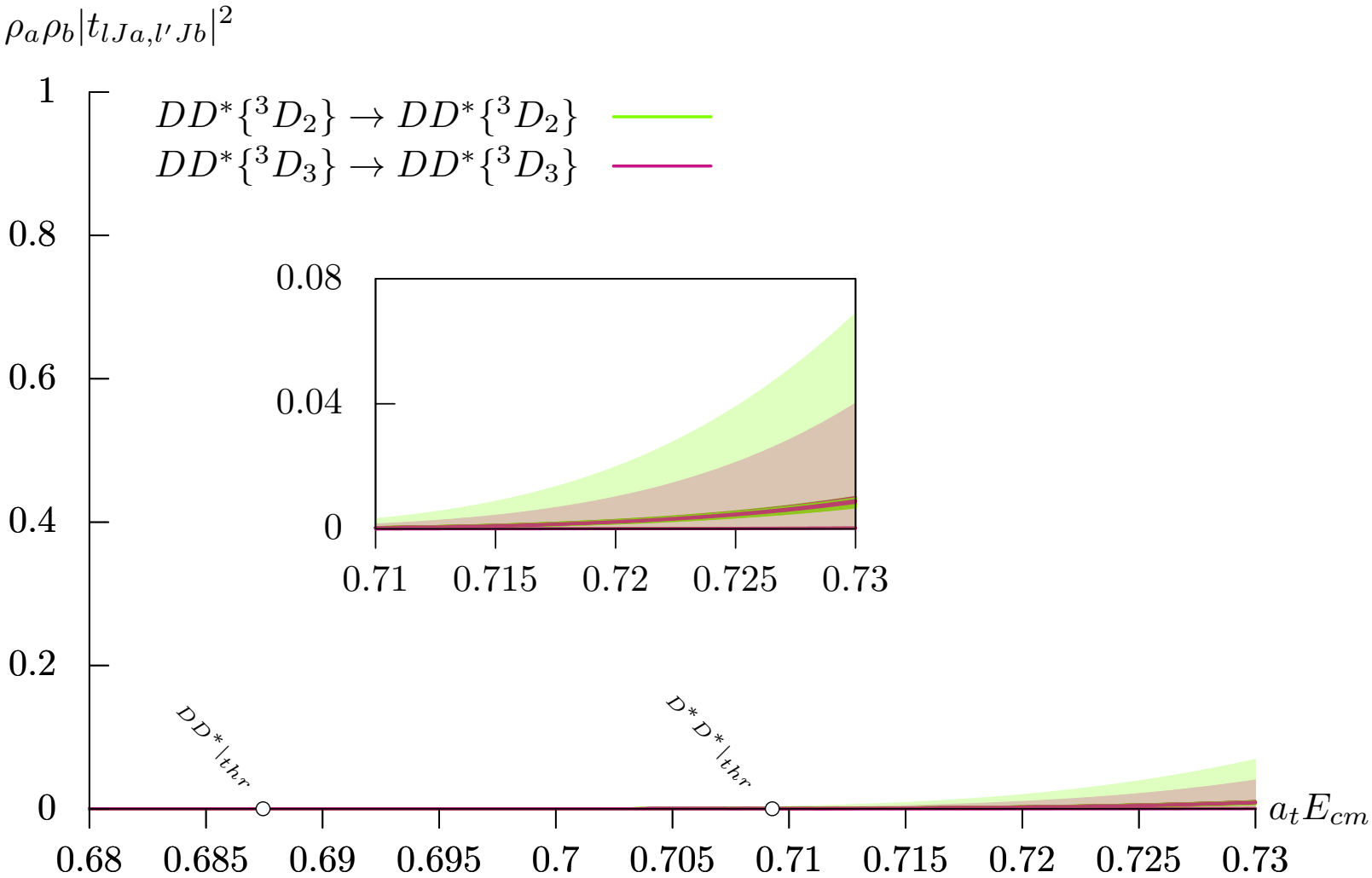

Parameterized Finite Volume Spectrum

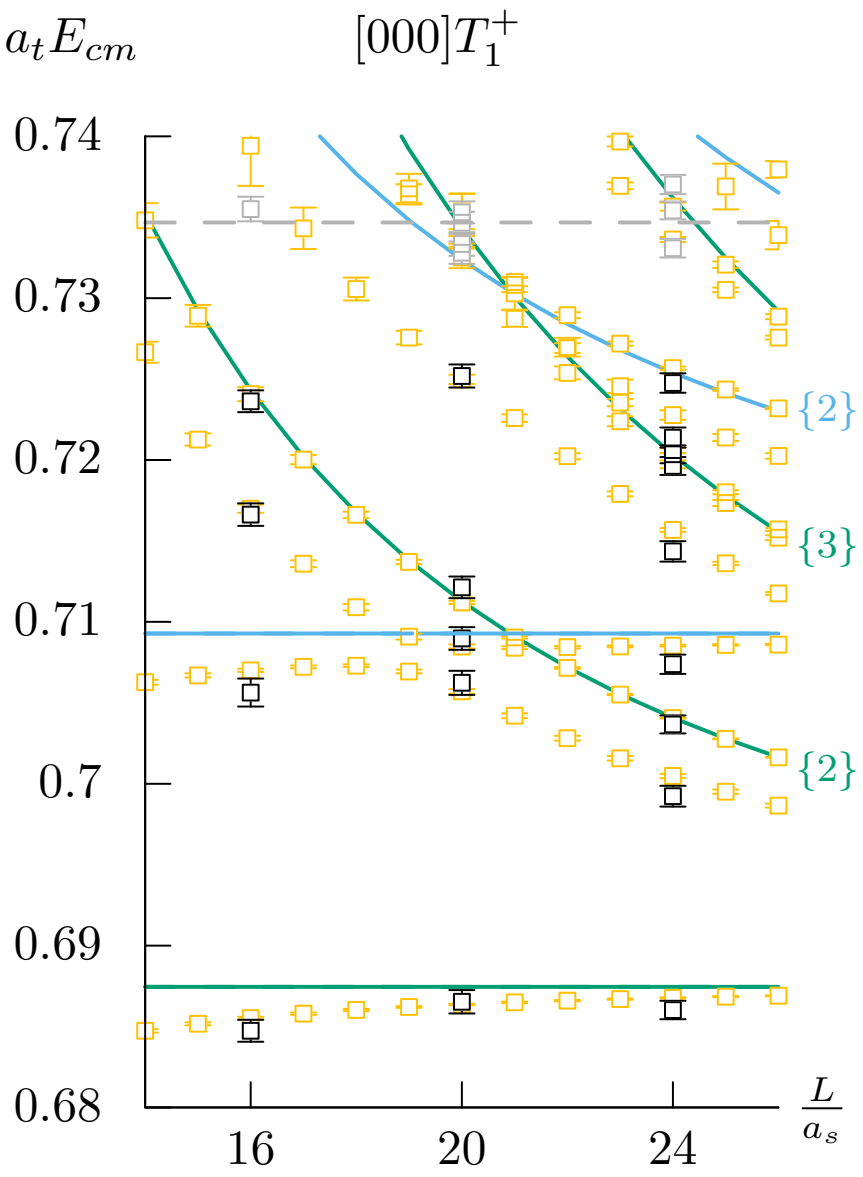

Resonance Poles

- At energies close to the position of a pole, the infinite volume scattering t-matrix takes on the form

$$t_{ij} \sim \frac{c_i c_j}{s_{pole} - s} \tag{11}$$

  which allows us to factorize the residue into the couplings c_i and c_j of the pole to each hadron channel
- Poles are characterized by their mass and width

$$\sqrt{s_{pole}} = m \pm \frac{i}{2}\Gamma \tag{12}$$

- A pole's influence on physical scattering determined by distance to physical scattering and can be observed in the complex momentum plane

Resonance Poles

- In coupled channel scattering, there are 4 Riemann sheets
- The four sheets in the s-plane can be unfolded to a single sheet by using $k_{D^*D^*}$ as a "uniformizing variable" Newton, Journal of Mathematical Physics 2 188, Morgan and Pennington Phys. Rev. D48 1185

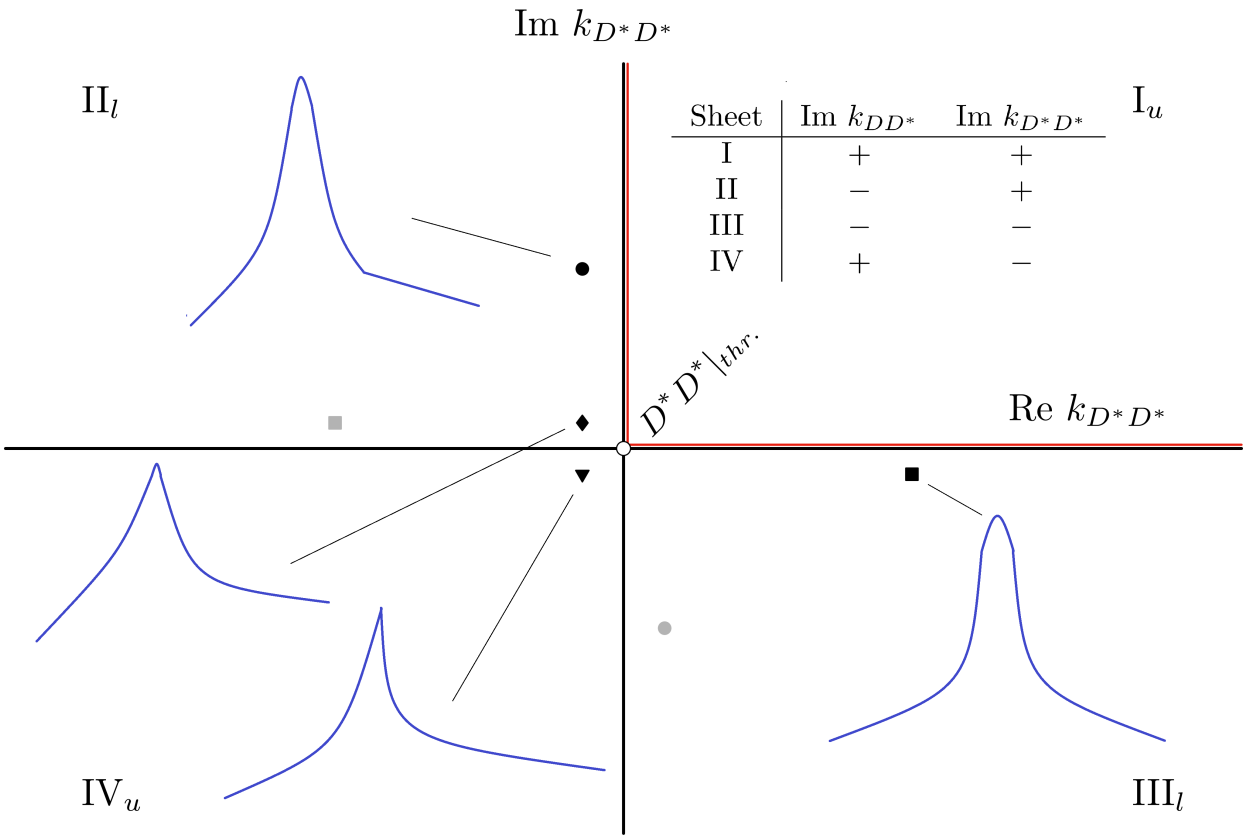

Varying the $DD^* \to D^*D^*$ S-wave Amplitude

What about the sheet II and III poles?

	Sheet II		Sheet III	
$\gamma^{(0)}_{DD^*\{^3S_1\}\to D^*D^*\{^3S_1\}}$	$\mathrm{Im}(k_{DD^*})$	$\mathrm{Im}(k_{D^*D^*})$	$\mathrm{Im}(k_{DD^*})$	$\mathrm{Im}(k_{D^*D^*})$
4.11	**-0.0493(36)**	**0.1003(18)**	**-0.0529(43)**	**-0.1021(22)**
3.60	-0.0480(35)	0.0996(17)	-0.0507(39)	-0.1010(20)
3.08	-0.0469(34)	0.0991(16)	-0.0489(37)	-0.1001(18)
2.57	-0.0460(32)	0.0987(15)	-0.0473(33)	-0.0993(16)
2.06	-0.0453(31)	0.0984(14)	-0.0461(31)	-0.0988(15)
1.54	-0.0448(31)	0.0981(14)	-0.0452(31)	-0.0983(14)
1.02	-0.0444(30)	0.0980(14)	-0.0446(30)	-0.0980(14)
0	-0.0441(32)	0.0978(14)	-0.0441(32)	-0.0978(14)

- Differences between sheet II and III poles resolve as the channels are decoupled: the sheet III pole becomes an exact mirror pole of sheet II pole
- We prescribe it no physical significance due to its distance from the physical sheet